In-plane strain control of the magnetic remanence and cation-charge redistribution in $CoFe_2O_4$ thin film grown on a piezoelectric substrate

Jung H. Park,[1] Jung-Hoon Lee,[1] Min G. Kim,[2] Young Kyu Jeong,[1] Min-Ae Oak,[1] Hyun Myung Jang,[1,*] Hyoung Joon Choi,[3] and James F. Scott[4]

[1]*Department of Materials Science and Engineering, and Division of Advanced Materials Science, Pohang University of Science and Technology (POSTECH), Pohang 790-784, Republic of Korea*

[2]*Pohang Accelerator Laboratory, Pohang University of Science and Technology (POSTECH), Pohang 790-784, Republic of Korea*

[3]*Department of Physics and IPAP, Yonsei University, Seoul 120-749, Republic of Korea*

[4]*Department of Physics, Cavendish Laboratory, University of Cambridge, Cambridge CB30HE, United Kingdom*

(Received 11 January 2010; published 1 April 2010)

Strain engineering of the magnetic property is an important subject in the study of multiferroic materials. Here we propose a multiferroic bilayer structure in which the magnetic remanence is controlled by the in-plane strain of the top CFO ($CoFe_2O_4$) layer epitaxially constrained by the bottom $Pb(Mg_{1/3}Nb_{2/3})O_3$-$PbTiO_3$ piezoelectric substrate. We have shown that the room-temperature magnetic remanence (M_R) of the 100-nm-thick CFO layer is enhanced by 35.4% when an electric field of 10 kV/cm is applied. The M_R value of our bilayer structure was shown to be linearly proportional to the magnitude of the in-plane compressive strain which, in turn, was proportional to the applied field strength. Synchrotron x-ray absorption near-edge structure study supports a scenario of the cation-charge redistribution between Co^{2+} and Fe^{3+} ions under the condition of an electric-field-induced in-plane compressive strain.

DOI: 10.1103/PhysRevB.81.134401 PACS number(s): 75.80.+q

I. INTRODUCTION

Multiferroic materials combine two or more of the properties of antiferromagnetism (or ferromagnetism), ferroelectricity, and ferroelasticity. In multiferroics, ferroelectric polarization is induced by an external magnetic field and an external electric field can induce changes in magnetization.[1] Multiferroism is currently the subject of intensive scientific investigation[1–10] because of the capability of showing a cross coupling between the ferromagnetic and ferroelectric order parameters, which possibly yields entirely new device paradigms.[7–9] However, there are few multiferroic systems existing in nature at room temperature because transition-metal *d* electrons reduce the tendency of an off-centering ferroelectric distortion.[1,6] The rareness of room-temperature multiferroics[2] has then led many workers to combine ferroelectric materials with ferromagnetic phases at microscopic or nanoscopic scales, for examples, nanoparticulate composite films,[11–14] multilayered thin films,[15] and nanopillar or columnar film structures.[16–19] In these dissimilar two-phase systems, magnetoelectric (ME) coupling effects can be considered as arising from the interfacial strain-mediated coupling of piezoelectricity and magnetostriction.

Among these two-phase composite structures, nanopillar or columnar structure is conceptually novel and seems to be the most promising approach in viewpoint of the ME coupling. The study of self-assembled ferroelectric-ferromagnetic nanopillar structures was pioneered by Zheng *et al.*[16] They reported the fabrication of three-dimensional nanopillar structure, where vertically aligned $CoFe_2O_4$ spinel nanopillars were embedded in a ferroelectric $BaTiO_3$ matrix. According to their assertion, these vertically aligned nanopillars undergo a strong interfacial ME coupling.[16] However, they did not present quantitative data that clearly support the interfacial ME coupling. Combining magnetic-force microscopy study with the technique of piezoelectric force microscopy, they later showed a direct evidence of the ME coupling by demonstrating the magnetization reversal induced by an electric field in epitaxial $BiFeO_3$-$CoFe_2O_4$ columnar nanostructures.[17] The estimated value of the static ME susceptibility, however, is not unusually large ($\chi_{ME} \approx 1.0 \times 10^{-2}$ G cm/V),[17] which is only slightly higher than that of a $CoFe_2O_4$-dispersed $Pb(Zr,Ti)O_3$ bulk composite (7.1×10^{-3} G cm/V).[20] Moreover, the processing of nanopillar or columnar structure is not simple, in general, to be readily adapted to a wide variety of multiferroic composites.[19]

Here we propose a multiferroic bilayer structure in which the magnetic response is controlled by the in-plane compressive strain of the top-layer epitaxially constrained by the bottom piezoelectric substrate. Figure 1 schematically depicts a ferromagnetic-piezoelectric asymmetric bilayer structure in which a single-crystalline $0.72Pb(Mg_{1/3}Nb_{2/3})O_3$

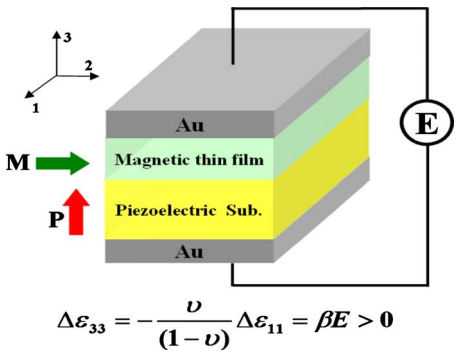

FIG. 1. (Color online) A schematic of a ferromagnetic/piezoelectric bilayer structure in which the magnetic remanence (M_R) is controlled by the *E*-field-induced in-plane strain of the top CFO layer epitaxially constrained by the bottom PMN-PT piezoelectric substrate.

$-0.28PbTiO_3$ (PMN-PT) solid solution is used as the bottom piezoelectric layer inasmuch as the PMN-PT at this composition is known to exhibits a giant piezoelectric response (~1700 pC/N).[21] In this asymmetric bilayer structure, an electric-field-induced giant piezoelectric strain from the bottom piezoelectric structure is effectively transferred to the top magnetostrictive layer epitaxially grown on this bottom PMN-PT substrate. In this way, an epitaxially grown $CoFe_2O_4$ (CFO) top layer is likely to exhibit a pronounced change in its magnetic remanence under a bias electric field because of (i) a giant induced strain imposed by an epitaxial constraint and (ii) a large inverse magnetostrictive effect arising from this induced strain.

II. EXPERIMENTAL DETAILS

A 100-nm-thick CFO top layer was grown on a PMN-PT(001) substrate by employing pulsed laser deposition method. KrF excimer laser (wavelength 248 nm; Lambda Physik) was used for this purpose. The deposition was carried out at 700 °C under $P_{O2}=10$ mTorr. To control the degree of the electric-field-induced strain, both top and bottom surfaces of the CFO/PMN-PT bilayer were coated with nonmagnetic Au films using a magnetron dc sputtering system.

For structural characterizations of the top layer, high-resolution x-ray diffraction patterns were obtained using a triple-axis x-ray diffractometer (X'pert PRO-MRD, Philips Inc.). Magnetization responses of the bilayer were examined by measuring magnetization-field (M-H) hysteresis curves using a superconducting quantum interference devices magnetometer (MPMS-5S; Quantum Design). The magnetic field was applied along the in-plane direction which is perpendicular to the direction of the applied electric field across the CFO/PMN-PT bilayer structure.

For a possible correlation of the in-plane compressive strain with the electronic states of constituting magnetic ions, we have carefully measured x-ray absorption near edge structure (XANES) spectra using a specially installed sample stage in the synchrotron 7C1 beam line of the Pohang Light Source (PLS). The fluorescence mode was used for the measurement. To remove possible extended x-ray-absorption fine structure (EXAFS) signals from an electrode surface, we have carefully chosen a conducting carbon layer as the top electrode.

III. RESULTS AND DISCUSSION

A. Epitaxial growth of the CFO layer on PMN-PT

Figure 2(a) represents a theta-2theta x-ray diffraction (XRD) pattern of the 100-nm-thick CFO thin film grown on a (001) PMN-PT single-crystalline substrate. The XRD pattern shows two strong diffraction peaks caused by the CFO layer: one at $2\theta=42.53°$ from CFO(004) and the other at $2\theta=93.1°$ from CFO(008), indicating that the CFO layer is preferentially grown along [001]. As shown in Fig. 2(b), the phi(Φ)-scan spectrum of the CFO layer on (202) is characterized by a fourfold symmetry and matches well with that of the PMN-PT substrate on its (101). The observed fourfold symmetry of the CFO layer is consistent with the expected

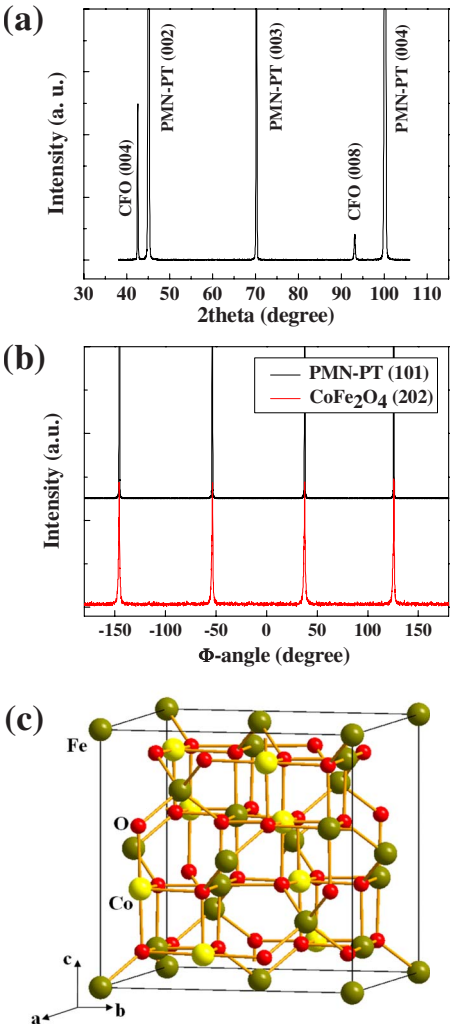

FIG. 2. (Color online) (a) Theta-2theta (θ-2θ) XRD pattern of the 100-nm-thick CFO thin film grown on a piezoelectric (001) PMN-PT substrate. (b) (101) phi(Φ)-scan diffraction spectra of the [001]-oriented CFO layer and the PMN-PT substrate. (c) Crystal structure of cubic inverse spinel, $CoFe_2O_4$.

fourfold symmetry of the cubic spinel structure [Fig. 2(c)]. Thus, the CFO layer has a homogeneous in-plane orientation and undergoes a coherent epitaxial growth on the (001) PMN-PT substrate.

The degree of the epitaxial misfit strain was examined by performing the (101) reciprocal space mapping (RSM) experiment using $2\theta-\omega$ scan. The percent misfit strain (Δ_i) can be related to the two relevant reciprocal scattering vectors:[14] $\Delta_i=(\mathbf{Q}_{i(S)}-\mathbf{Q}_{i(F)})/\mathbf{Q}_{i(F)}\times 100$, where the subscript "$i$" stands for either x (in-plane direction) or z (out-of-plane direction) and the subscripts "S" and "F," respectively, denote the substrate and the film layer. As shown in Fig. 3, the difference in $\mathbf{Q}_x$ between the CFO layer and the substrate is essentially negligible, demonstrating an epitaxial constraint imposed on the CFO layer with a nearly zero value of the in-plane misfit strain (i.e., $\mathbf{Q}_{x(F)}=\mathbf{Q}_{x(S)}$). We have further estimated the in-plane and out-of-plane lattice parameters of the epitaxial CFO layer using the RSM data and the bulk lattice parameter of the cubic spinel CFO. They are 8.105 Å (in-plane) and

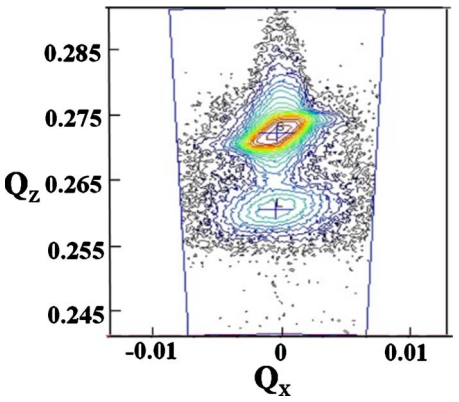

FIG. 3. (Color online) (101) reciprocal space mapping of the 100-nm-thick CFO film grown on a (001) PMN-PT.

8.397 Å (out-of-plane), respectively. This clearly indicates that the CFO film on a PMN-PT is compressively strained along the in-plane direction.

B. Electric-field-control of magnetic remanence and ME susceptibility

To experimentally isolate the effect of the electric (E)-field-induced in-plane strain on the variation in the magnetic response of the CFO layer, we have measured the magnetization-field (M-H) hysteresis loop under a bias E field and compared this with the M-H hysteresis loop obtained without applying any external E field. The magnetic field was applied along the in-plane direction which is perpendicular to the direction of the applied E field across the CFO/PMN-PT bilayer structure. As shown in Fig. 4(a), the room-temperature magnetic remanence (M_R) of the CFO layer is enhanced by 35.4% when an E field of 10kV/cm is applied. M_R increases almost linearly with the E-field strength up to 10 kV/cm [Fig. 4(b)]. Interestingly, this E-field dependence of M_R is reproducible and reversible. Thus, the M_R value can be suitably controlled by adjusting the E-field strength. The observed linear augmentation of M_R with the E-field strength suggests that the increase in the in-plane compressive strain (vertical to the E-field direction) in response to the applied E field enhances M_R of the top CFO layer which is epitaxially constrained by the bottom piezoelectric PMN-PT substrate.

The static ME coupling susceptibility[17] of the CFO/PMN-PT bilayer structure was evaluated using the observed change in M_R [inset of Fig. 4(a)].

$$\chi_{\mathrm{ME}} = \frac{\{M_R(E) - M_R(0)\}}{E} \equiv \frac{\Delta M_R}{E} \approx 5.29 \times 10^{-3}\ \text{emu/Vcm}^2 = 6.65 \times 10^{-2}\ \text{G cm/V}. \quad (1)$$

This value of χ_{ME} is more than six times higher than the largest previously reported value of χ_{ME} ($\approx 1.0 \times 10^{-2}$ G cm/V) found in epitaxial $BiFeO_3$-$CoFe_2O_4$ columnar structures.[17] The pronounced ME coupling suggests

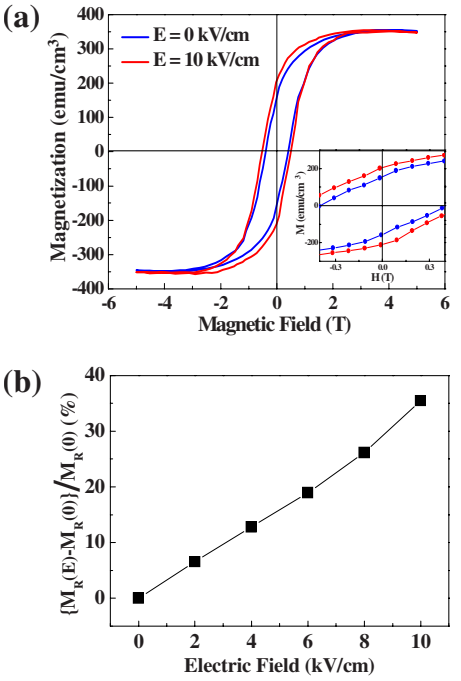

FIG. 4. (Color online) (a) Room-temperature magnetization-field (M-H) hysteresis curves of the CFO thin film epitaxially grown on a (001) PMN-PT substrate with and without applying a bias E field along [001]. (b) The relative change in the magnetic remanence of the CFO layer plotted as a function of the bias E-field strength.

that an E-field-induced giant piezoelectric strain from the PMN-PT substrate is effectively transferred to the magnetostrictive CFO layer which is epitaxially constrained by the bottom piezoelectric substrate.

C. Magnetic remanence versus electric-field-induced in-plane strain

Having correlated the change in M_R with the applied E-field strength, we now examine the observed variation of M_R in terms of the E-field-induced in-plane strain. This will clarify our proposition stated previously that an E-field-induced piezoelectric strain from the PMN-PT substrate is effectively transferred to the epitaxially constrained CFO layer, thereby increasing M_R of this magnetostrictive layer. To do this, we first examined the variation in the out-of-plane lattice parameter of the CFO layer as a function of the bias E field along [001]. As shown in the XRD pattern [Fig. 5(a)], the CFO(004) peak shifts to a lower 2theta angle with increasing E-field strength. This demonstrates that the E-field-induced in-plane compressive strain in the piezoelectric PMN-PT substrate is transferred to the top CFO layer and thus increases the out-of-plane lattice parameter of the epitaxially constrained CFO layer.

The variation in the E-field-induced out-of-plane strain ($\Delta\varepsilon_{33}$) was estimated using the following relation:[22] $\Delta\varepsilon_{33} = [a_{001}(E) - a_{001}(0)]/a_{001}(0) = [a_{004}(E) - a_{004}(0)]/a_{004}(0)$, where $a_{001}(E)$ and $a_{001}(0)$, respectively, are the (001) lattice parameters of the CFO layer at an E-field strength E and

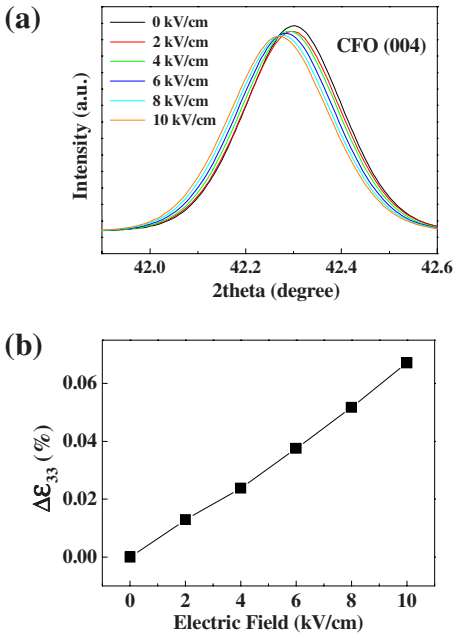

FIG. 5. (Color online) (a) *In situ* theta-2theta XRD(004) peaks of the epitaxially grown CFO layer (100-nm thick) under various *E*-field strengths. (b) The *E*-field-induced out-of-plane strain of the CFO layer plotted as a function of the applied *E*-field strength.

under a zero-field condition. As shown in Fig. 5(b), $\Delta\varepsilon_{33}$ increases almost linearly with the *E*-field strength up to 10 kV/cm. The positive value of $\Delta\varepsilon_{33}$ signifies that the out-of-plane lattice parameter of the CFO layer increases with the *E* field applied along the [001] direction. On the other hand, the in-plane lattice parameter of the constrained CFO layer is expected to be reduced with the *E*-field strength as the applied *E* field induces a compressive strain in the PMN-PT substrate along the in-plane direction.

The induced in-plane compressive strain ($\Delta\varepsilon_{11}=\Delta\varepsilon_{22}$) developed along the direction perpendicular to the applied *E* field can be estimated using the following relation:

$$\Delta\varepsilon_{33} = -\frac{\upsilon}{(1-\upsilon)}\Delta\varepsilon_{11}, \tag{2}$$

where υ is Poisson's ratio. The induced in-plane strain ($\Delta\varepsilon_{11}$) in the CFO layer was estimated using Eq. (2) with $\upsilon=0.333$ for the CFO film.[23] According to Fig. 4(b), the *E*-field-induced M_R can be written as $\{M_R(E)-M_R(0)\}/M_R(0) \equiv \Delta M_R/M_R = \alpha E$, where α is a positive constant. On the other hand, the induced out-of-plane strain can be quantified by $\Delta\varepsilon_{33}=\beta E$ [Fig. 5(b)], where β is another positive constant. Using these two empirical relations and Eq. (2), one can obtain the following relation:

$$\frac{\{M_R(E)-M_R(0)\}}{M_R(0)} \equiv \frac{\Delta M_R}{M_R} = \gamma\Delta\varepsilon_{11}, \tag{3}$$

where γ is defined as $-(\alpha/\beta)\cdot\{\upsilon/(1-\upsilon)\}<0$. Thus, Eq. (3) predicts that plotting $\Delta M_R/M_R$ with respect to $\Delta\varepsilon_{11}$ yields a linear line with the slope being negative. As shown in Fig. 6, $\Delta M_R/M_R$ is indeed proportional to $\Delta\varepsilon_{11}$ of the CFO layer. When a bias *E* field of 10 kV/cm is applied, the induced in-plain compressive strain is −0.136% with $\Delta M_R/M_R$ as high as 35.4%. Figure 6 clearly demonstrates that the M_R value of our bilayer structure is linearly correlated with $\Delta\varepsilon_{11}$ which, in turn, is proportional to the applied *E*-field strength.

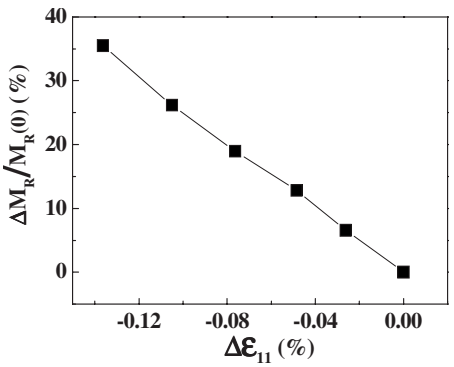

FIG. 6. Correlation of $\Delta M_R/M_R$ with the *E*-field-induced in-plane strain of the CFO layer epitaxially constrained by the bottom PMN-PT piezoelectric substrate.

D. First-principles study

The effect of the in-plane strain on M_R of the CFO layer was theoretically examined by applying density-functional theory (DFT) computations. To do this, we performed first-principles electronic-structure calculations on the basis of the local spin-density approximation and *ab initio* norm-conserving pseudopotentials[24,25] using the SIESTA code.[26] The calculated total magnetic moment of the unconstrained CFO with an inverse spinel structure is $3.0\mu_B$ per formula unit. Contrary to this, the calculated total magnetic moment of the constrained inverse spinel CFO using the experimental value of $\Delta\varepsilon_{11}(=-0.136\%)$ is as high as $4.5\mu_B$ per formula unit. Thus, the DFT magnetization qualitatively explains the observed enhancement of M_R under a compressively strained state.

We have further examined a possibility of the inverse-to-normal spinel transformation in a highly constrained CFO. In an unconstrained condition, the Kohn-Sham energy of the inverse spinel CFO is 1.35 eV lower than that of the normal spinel, which accords with the reported stability of the inverse phase.[27] The computed Kohn-Sham energy of the inverse spinel is also found to be lower than that of the normal spinel even in a highly constrained state with the difference of 1.16 eV at $\Delta\varepsilon_{11}=-0.136\%$. Thus, it is highly unlikely that the in-plane compressive strain invokes a structural instability of the inverse phase, expediting the formation of the normal spinel phase in the epitaxially constrained CFO layer.

E. Cation-charge redistribution

Finally, we have examined a possible correlation of the in-pane compressive strain with the electronic states of constituting magnetic ions (Co and Fe) in the constrained CFO layer. For this purpose, we have carefully monitored the effect of a bias *E* field on the XANES spectrum of the CFO layer using synchrotron 7C1 beamline of the PLS at Pohang Accelerator Laboratory. To remove possible EXAFS signals

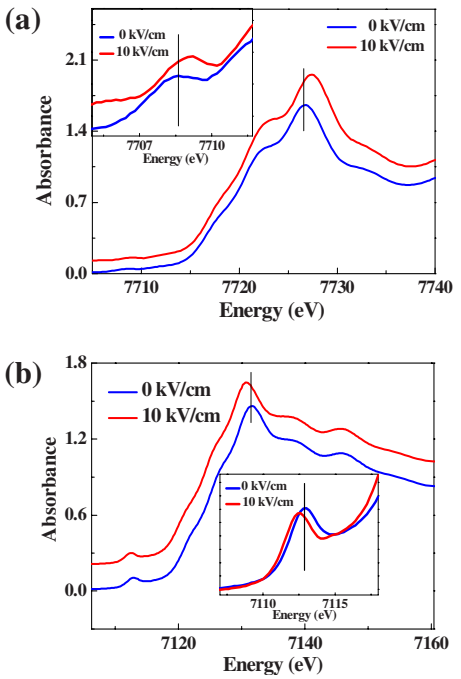

FIG. 7. (Color online) (a) Co and (b) Fe K-edge XANES spectra of the CFO thin film epitaxially grown on a (001) PMN-PT substrate with and without applying a bias E field along [001]. The inset shows a magnified view of the pre-edge region.

from an electrode surface, we have carefully chosen a conducting carbon layer as the top electrode. Figure 7(a) presents the Co K-edge XANES spectra of the constrained CFO layer with and without applying an E field along the out-of-plane [001] direction. As shown in inset of Fig. 7(a), a pre-edge peak (~7708 eV) moves toward a higher-energy region under an applied E field of 10 kV/cm. It is known that this pre-edge peak which corresponds to a $1s \rightarrow 3d$ forbidden electronic transition reflects the oxidation state of Co.[28] A detailed XANES study using several cobalt oxide reference compounds indicates that the pre-edge position of Co^{3+} is higher than that of Co^{2+}.[28,29] As shown in Fig. 7(a), the threshold energy corresponding to the main peak (marked with a vertical bar) also shifts to a higher energy when a bias E field is applied along [001]. Thus, it can be concluded that the divalent Co^{2+} ions in the CFO layer partly oxidize to a higher valence state ($2+\delta$, where $\delta \ll 1$) under the condition of an E-field-induced in-plane compressive strain.

Contrary to the case of the Co K-edge spectrum, both the main and pre-edge peaks of the Fe K-edge XANES spectrum move toward lower-energy regions when a bias E field is applied [Fig. 7(b)]. It is known that the K-edge threshold energy corresponding to the trivalent Fe^{3+} state is higher than that of the divalent Fe^{2+} state with the difference of about 5 eV.[30] Therefore, the observed shift of the K-edge threshold peak to a lower-energy region indicates that the trivalent Fe^{3+} ion partially reduces its oxidation state to a lower valence value of $3-\delta$ under the condition of an E-field-induced in-plane compressive strain. From these XANES results, one can delineate a cation-charge-redistribution scenario that under the condition of an in-plane compressive strain, Fe^{3+} ion partially reduces its oxidation state while Co^{2+} ion partially oxidizes to a higher valence state, $2+\delta$. The cation-charge redistribution suggests a partial transfer of $3d$ electrons from the triply degenerated t_{2g} orbitals of a high-spin Co^{2+} to the half-filled $3d$ orbitals of a high-spin Fe^{3+}. This partial charge redistribution possibly modulates the strength of the exchange interaction between Fe and Co spins in the inverse spinel, $Fe^{3+}(Co^{2+}Fe^{3+})$.

The in-plane-distortion-induced partial charge transfer then possibly activates a fully quenched orbital momentum ($\boldsymbol{L}=0$) of the half-filled Fe^{3+} ions.[31] The orbital angular momentum contribution to the total magnetic moment of the unquenched Co^{2+} ions is also known to be sensitive to the distortion of the ligand field.[32] Thus, the observed in-plane-strain-induced enhancement of M_R could be partly attributed to a nonspin contribution: (i) the activation of a fully quenched orbital momentum (Fe^{3+}) or (ii) the modulation of an unquenched (or partially quenched) orbital momentum (Co^{2+}) via the cation-charge redistribution.

IV. CONCLUSIONS

We have presented a multiferroic bilayer structure in which the magnetic remanence is controlled by the in-plane strain of the top CFO layer epitaxially constrained by the bottom PMN-PT piezoelectric substrate. We have shown that the room-temperature magnetic remanence (M_R) of the CFO layer is enhanced by 35.4% when an E field of 10 kV/cm is applied. It has been further demonstrated that the M_R value of our bilayer structure is linearly correlated with the magnitude of the in-plane compressive strain which, in turn, is proportional to the applied E-field strength. *In situ* synchrotron XANES study supports a scenario of the partial cation-charge redistribution between Co^{2+} and Fe^{3+} ions under the condition of a bias E-field-induced in-plane compressive strain. This possibly modulates the strength of the exchange interaction between Fe and Co spins.

ACKNOWLEDGMENTS

This work was supported by the Korea Research Foundation (KRF) under Contract No. KRF-2008-313-C00252 and by Pohang Steel Corporation (POSCO) through *Steel Science Research Program* (Project No. 2009Y209).

*Author to whom correspondence should be addressed; hmjang@postech.ac.kr

[1] N. A. Hill, J. Phys. Chem. B **104**, 6694 (2000).
[2] J. Wang, J. B. Neaton, H. Zheng, V. Nagarajan, S. B. Ogale, B. Liu, D. Viehland, V. Vaithyanathan, D. G. Schlom, U. V. Waghmare, N. A. Spaldin, K. M. Rabe, M. Wuttig, and R. Ramesh, Science **299**, 1719 (2003).
[3] T. Kimura, T. Goto, H. Shintani, K. Ishizaka, T. Arima, and Y. Tokura, Nature (London) **426**, 55 (2003).
[4] N. Hur, S. Park, P. A. Sharma, J. S. Ahn, S. Guha, and S. W. Cheong, Nature (London) **429**, 392 (2004).
[5] S. M. Selbach, T. Tybell, M.-A. Einarsrud, and T. Grande, Chem. Mater. **19**, 6478 (2007).
[6] R. Seshadri and N. A. Hill, Chem. Mater. **13**, 2892 (2001).
[7] N. A. Spaldin and M. Fiebig, Science **309**, 391 (2005).
[8] W. Eerenstein, N. D. Mathur, and J. F. Scott, Nature (London) **442**, 759 (2006).
[9] Y. Tokura, Science **312**, 1481 (2006).
[10] S. Ishiwata, Y. Taguchi, H. Murakawa, Y. Onose, and Y. Tokura, Science **319**, 1643 (2008).
[11] J. G. Wan, X. W. Wang, Y. J. Wu, M. Zeng, Y. Wang, H. Jiang, W. Q. Zhou, G. H. Wang, and J.-M. Liu, Appl. Phys. Lett. **86**, 122501 (2005).
[12] H. Ryu, P. Murugavel, J. H. Lee, S. C. Chae, T. W. Noh, Y. S. Oh, H. J. Kim, K. H. Kim, J. H. Jang, M. Kim, C. Bae, and J.-G. Park, Appl. Phys. Lett. **89**, 102907 (2006).
[13] X. L. Zhong, J. B. Wang, M. Liao, G. H. Huang, S. H. Xie, Y. C. Zhou, Y. Qiao, and J. P. He, Appl. Phys. Lett. **90**, 152903 (2007).
[14] J. H. Park, H. H. Shin, and H. M. Jang, Phys. Rev. B **77**, 212409 (2008).
[15] S. Ryu, J. H. Park, and H. M. Jang, Appl. Phys. Lett. **91**, 142910 (2007).
[16] H. Zheng, J. Wang, S. E. Lofland, Z. Ma, L. Mohaddes-Ardabili, T. Zhao, L. Salamanca-Riba, S. R. Shinde, S. B. Ogale, F. Bai, D. Viehland, Y. Jia, D. G. Schlom, M. Wuttig, A. Roytburd, and R. Ramesh, Science **303**, 661 (2004).
[17] F. Zavaliche, H. Zheng, L. Mohaddes-Ardabili, S. Y. Yang, Q. Zhan, P. Shafer, E. Reilly, R. Chopdekar, Y. Jia, P. Wright, D. G. Schlom, Y. Sizuki, and R. Ramesh, Nano Lett. **5**, 1793 (2005).
[18] Y. G. Ma, W. N. Cheng, M. Ning, and C. K. Ong, Appl. Phys. Lett. **90**, 152911 (2007).
[19] N. Dix, R. Muralidharan, B. Warot-Fonrose, M. Varela, F. Sánchez, and J. Fontcuberta, Chem. Mater. **21**, 1375 (2009).
[20] J. H. Park, M. G. Kim, S.-J. Ahn, S. Ryu, and H. M. Jang, J. Magn. Magn. Mater. **321**, 1971 (2009).
[21] Y. Jia, S. W. Or, H. L. W. Chan, X. Zhao, and H. Luo, Appl. Phys. Lett. **88**, 242902 (2006).
[22] R. K. Zheng, Y. Wang, H. L. W. Chan, C. L. Choy, and H. S. Luo, Phys. Rev. B **75**, 212102 (2007).
[23] A. Lisfi, C. M. Williams, L. T. Nguyen, J. C. Lodder, A. Coleman, H. Corcoran, A. Johnson, P. Chang, A. Kumar, and W. Morgan, Phys. Rev. B **76**, 054405 (2007).
[24] M. L. Cohen, Phys. Scr. **T1**, 5 (1982).
[25] N. Troullier and J. L. Martins, Phys. Rev. B **43**, 1993 (1991).
[26] D. Sánchez-Portal, P. Ordejón, E. Artacho, and J. M. Soler, Int. J. Quantum Chem. **65**, 453 (1997).
[27] Z. Szotek, W. M. Temmerman, D. Ködderitzsch, A. Svane, L. Petit, and H. Winter, Phys. Rev. B **74**, 174431 (2006).
[28] S. Ammar, A. Helfen, N. Jouini, F. Fiévet, I. Rosenman, F. Villain, P. Molinié, and M. J. Danot, J. Mater. Chem. **11**, 186 (2001).
[29] M. G. Kim and C. H. Yo, J. Phys. Chem. B **103**, 6457 (1999).
[30] S. Sasaki, Rev. Sci. Instrum. **66**, 1573 (1995).
[31] J.-Y. Kim, T. Y. Koo, and J.-H. Park, Phys. Rev. Lett. **96**, 047205 (2006).
[32] G. Juhász, R. Matsuda, S. Kanegawa, K. Inoue, O. Sato, and K. J. Yoshizawa, J. Am. Chem. Soc. **131**, 4560 (2009).